338 *Chem. Mater.* **2010,** *22,* 338–346
DOI:10.1021/cm902528y

CHEMISTRY OF MATERIALS
Article

Novel Large-Pore Aluminophosphate Molecular Sieve STA-15 Prepared Using the Tetrapropylammonium Cation As a Structure Directing Agent

Zhongxia Han,[†] A. Lorena Picone,[†] Alexandra M.Z. Slawin,[†] Valerie R. Seymour,[†] Sharon E. Ashbrook,[†] Wuzong Zhou,[†] Stephen P. Thompson,[‡] Julia E. Parker,[‡] and Paul A. Wright*,[†]

[†]*School of Chemistry, University of St Andrews, Purdie Building, North Haugh, St. Andrews, Fife, KY16 9ST, United Kingdom and* [‡]*Diamond Light Source, Harwell Science and Innovation Campus, Didcot, Oxfordshire OX11 0DE, United Kingdom*

Received August 17, 2009. Revised Manuscript Received October 12, 2009

The novel aluminophosphate STA-15 (St Andrews microporous solid-15) is prepared by hydrothermal synthesis in the presence of tetrapropylammonium hydroxide (TPAOH), which acts as a structure directing agent. The crystallization is accelerated by the addition of low concentrations of tetraphenylphosphonium or other bulky organic cations, and the purity is improved by the addition of silica to the gel, but these additives are not included in the final crystalline product. The structure of STA-15 was solved by a combination of synchrotron X-ray powder diffraction and modeling. The as-prepared form of STA-15 (*Iba2*, a = 14.7953(1) Å, b = 27.3634(3) Å, c = 8.34464(6) Å at 100 K) has unit cell composition $Al_{32}P_{32}O_{128}(OH)_{1.8}TPA_{1.8}\cdot 3H_2O$. It has a system of one dimensional channels, limited by strongly elliptical 12-membered rings (12 tetrahedral cations and 12 oxygen atoms, 8.7 × 5.7 Å) in which the TPA^+ cations reside. The charge-balancing hydroxide ions are coordinated to framework Al, as shown by ^{27}Al and ^{31}P MAS NMR. STA-15 is stable to removal of the organic and hydroxyl species upon calcination in oxygen, leaving a microporous solid with a pore volume of 0.11 $cm^3\ g^{-1}$ and showing uptakes of *n*-hexane and toluene (at 297 K, p/p_o = 0.10) of 0.48 and 0.69 mmol g^{-1}, respectively.

Introduction

Microporous inorganic solids with zeolitic properties are of great importance as sorbents and catalysts and have high potential in emerging technologies.[1,2] Among these solids, aluminosilicates, silicas and aluminophosphates with tetrahedrally-connected frameworks are of most general interest, because of their high thermal stability and properties as catalysts. For aluminophosphate-based molecular sieves,[3−7] the inclusion of Mg for Al, or Si for P, introduces acidity for solid acid catalysts,[1,5,8,9] and the inclusion of redox metals, such as Mn, Co, or Fe, for Al produces redox active solids suitable for selective oxidation catalysis.[1,10−12] Although the mechanism of the crystallization of zeolites and aluminophosphates remains an open question of current interest,[13,14] the role of inorganic and organic species as structure directing agents, or templates, is of fundamental importance. Indeed, for the aluminophosphate solids, first discovered by Wilson, Lok, and Flanigen et al.,[3−6] all of the most porous frameworks are prepared in the presence of organic amines or alkylammonium cations that are occluded in the solid after crystallization, and must be removed by calcination in oxygen to render the solids porous. As a result, there is particular interest in those materials that can be prepared using readily available organic species, and initial synthetic efforts concentrated on the use of tetraalkylammonium cations (NR_4^+, where R = CH_3, C_2H_5, C_3H_7, and C_4H_9). The tetrapropylammonium cation (TPA^+) has been reported to act as a structure directing agents for the aluminophosphates $AlPO_4$-5 and $AlPO_4$-40 (the latter favored by the presence of low

*To whom correspondence should be addressed. E-mail: paw2@st-andrews.ac.uk. Tel: (0)1334 463793. Fax: (0)1334 463808.

(1) Wright, P. A. *Microporous Framework Solids*; RSC Publishing: Cambridge, U.K., 2007
(2) Davis, M. E. *Nature* **2002**, *417*, 813.
(3) Wilson, S.T.; Lok, B. M.; Messina, C. A.; Cannan, T. R.; Flanigen, E. M. *J. Am. Chem. Soc.* **1982**, *104*, 1146.
(4) Wilson, S. T.; Lok, B. M.; Flanigen, E. M. U.S. Patent 4,310,440, **1982**
(5) Lok, B. M.; Messina, C. A.; Patton, R. L.; Gajek, R. T.; Cannan, T. R.; Flanigen, E. M. *J. Am. Chem. Soc.* **1984**, *106*, 6092.
(6) Lok, B. M.; Messina, C. A.; Patton, R. L.; Gajek, R. T.; Cannan, T. R.; Flanigen, E. M. U.S. Patent 4,440,871, **1984**
(7) Patarin, J.; Paillaud, J. L.; Kessler, H. In *Handbook of Porous Solids*; Schuth, F., Sing, K. S. W., Weitkamp, J., Eds.; Wiley-VCH: New York, 2002; p 815.
(8) Haw, J. F.; Song, W.; Marcus, D. M.; Nicholas, J. B. *Acc. Chem. Res.* **2003**, *36*, 317.
(9) Wright, P. A.; Sayag, C.; Rey, F.; Lewis, D. W.; Gale, J. D.; Natarajan, S.; Thomas, J. M. *J. Chem. Soc. Faraday Trans.* **1995**, *91*, 3537.
(10) Thomas, J. M.; Raja, R.; Sankar, G.; Bell, R. G. *Acc. Chem. Res.* **2001**, *34*, 191.
(11) Thomas, J. M.; Raja, R. *Proc. Natl. Acad. Sci. U. S. A.* **2005**, *102*, 13732.
(12) Raja, R.; Thomas, J. M.; Xu, M. C.; Harris, K. D. M.; Greenhill-Cooper, M.; Quill, K. *Chem. Commun.* **2006**, 448.
(13) O'Brien, M. G.; Beale, A. M.; Catlow, C. R. A.; Weckhuysen, B. M. *J. Am. Chem. Soc.* **2006**, *128*, 11744.
(14) Cubillas, P.; Castro, M.; Jelfs, K. E.; Lobo, A. J. W.; Slater, B.; Lewis, D. W.; Wright, P. A.; Stevens, S. M.; Anderson, M. W. *Cryst. Growth Des.* **2009**, *9*, 4041.

 Published on Web 12/18/2009

Table 1. Gel Compositions (Molar Ratios) and Resultant Products for Hydrothermal Syntheses of STA-15[a]

$Al(OH)_3$	H_3PO_4	SiO_2	$Co(Ac)_2$	TPA^+	TPP^+	K222	H_2O	product (PXRD label, Figure 1)
1	1			0.64			70	STA-15 + $AlPO_4$-5 (a)
0.9	1			0.64			70	STA-15 + impurity (b)
0.9	1	0.2		0.64			70	poorly crystalline STA-15 (c)
0.9	1	0.2		0.64	0.108	0.008	70	STA-15 (d)
0.9	1			0.64			70	STA-15 + minor impurity (e)
0.9	1	0.2		0.64	0.108		70	STA-15 (f)
0.9	1	0.2		0.60			70	STA-15 (g)
0.9	1			0.64			36	$AlPO_4$-5 (h)
0.85	1	0	0.05	0.64			70	STA-15 + minor impurity[b]

[a] All preparations based on 6.24 mmol H_3PO_4. TPAOH added to give an initial pH of 6.5−7.0. This typically required TPA^+/P molar ratio of 0.60−0.64. All syntheses in the table were performed at 190 °C for 168 h. a−d in new PTFE liners, others in used liners washed with hot dilute nitric acid. [b] Preparation seeded with 0.04 mmol of as-prepared $AlPO_4$−STA-15.

levels of added tetramethylammonium TMA^+),[3,15] and the silicoaluminophosphates SAPO-5,[16] SAPO-40,[5,6,16] and SAPO-34,[17] where the product phase depends on the reaction conditions and presence of additives that are not included in the crystals. In addition, SAPO-37 is templated by a mixture of TPA^+ and TMA^+ cations, where both are included in the final product.[5,18] The ability of an organic molecule to be able to direct to more than one structure is well known in zeolites and related materials, the commercially available hexamethonium cation has recently been shown to give the novel aluminophosphate-based EMM-3[19] and had previously been shown to template the silicoaluminophosphate SAPO-17.[20]

In this paper, we report the synthesis of a novel large pore aluminophosphate, STA-15 (St. Andrews microporous material-15) using the tetrapropylammonium cation (TPA^+) as a structure directing agent. That a new material was obtained using reactants and conditions that had previously been investigated is remarkable, and underlines the critical dependence of phase formation on kinetic factors deriving from details of gel chemistry. The new solid was prepared during an ongoing program of research in which combinations of organic bases are examined for their co-templating abilities:[21] in the synthesis of STA-15, the addition of low concentrations of large charged molecules tetraphenylphosphonium (TPP^+) or the azaoxacryptand 4,7,13,16,21,24-hexaoxa-1,10-diazabicyclo[8.8.8]hexacosane (K222) along with TPA^+ results in the acceleration of crystallization, without their incorporation.

Experimental Section

Synthesis. Hydrothermal syntheses were performed by combining sources of potential framework species Al, P (and in some cases Si) with distilled water and organic additives. All reagents were used as supplied ($Al(OH)_3 \cdot 0.2\ H_2O$, Aldrich, 98%; H_3PO_4, Analar, 85% aq.; fumed SiO_2, Fluka, 97%; TPAOH, Aldrich 1M (aq); TPPBr, Aldrich, 97%; K222, ABCR, 97%; Cobalt acetate, $Co(Ac)_2 \cdot 4H_2O$, Aldrich). Details are given in Table 1. All gels were stirred at room temperature until homogeneous, then loaded in PTFE-lined stainless steel autoclaves and heated at 190 °C for 72 or 168 h. The initial experiments were performed in PTFE liners (23 mL capacity) that had not previously been used in the synthesis of aluminophosphates: subsequent reactions were performed in liners that were cleaned between syntheses by prolonged washing in hot dilute nitric acid. In the syntheses, after removing autoclaves from the oven and allowing them to cool, the reaction mixtures were suspended in water, and if necessary, the suspensions were sonicated to force separation of crystals from a suspension of amorphous material, which was decanted. In the case of the cobalt-containing preparation, larger crystals of an impurity phase were removed by resonication and exclusion of the coarsest fraction. The products were filtered, washed, and air dried at 60 °C.

Characterization and Structure Determination. Laboratory X-ray powder diffraction of the crystalline fraction of these samples was performed on a Stoe STADI P diffractometer, using monochromated Cu $K_{\alpha 1}$ X-radiation, over a period of 1 h. For structural studies, two pure samples of as-prepared STA-15, prepared in different ways (samples d and f of Table 1), were analyzed in Debye−Scherrer mode on beamline I11 at the Diamond Light Source at 100 K.[22] In addition, samples of the same two STA-15 materials were calcined at 550 °C for 12 h in flowing oxygen and then loaded into 0.5 mm quartz glass capillaries attached to a vacuum line, where they were dehydrated at 200 °C for 3 h to remove water and sealed under vacuum. One calcined and dehydrated sample (d) was analyzed at 290 K in Debye−Scherrer mode on a Stoe STADI P diffractometer, using monochromated Cu $K_{\alpha 1}$ X-radiation, over a period of 16 h. The other (f) was analysed in Debye-Scherrer mode at the Diamond Light Source at 100 K under the same conditions as its corresponding as-prepared material. Rietveld analysis of the data was performed using the GSAS suite of programs.[23]

A single crystal of $AlPO_4$ STA-15 (prepared after 3 days heating of a gel of type d in Table 1) was analyzed on a Rigaku diffractometer fitted with a rotating copper anode (Cu K_α, $\lambda = 1.54178$ Å) and a CCD detector (Supporting Information).

(15) Lourenco, J.P.; Ribeiro, M. F.; Ramoa Ribeiro, F.; Rocha, J.; Onida, B.; Garrone, E.; Gabelica, Z. *Zeolites* **1997**, *18*, 398.
(16) Dumont, N.; Gabelica, Z.; Derouane, E. G.; Di Renzo, F. *Microporous Mater*. **1994**, *3*, 71.
(17) Felix, D. L.; Strauss, M.; Ducati, L. C.; Pastore, H. O. *Microporous Mesoporous Mater*. **2009**, *120*, 187.
(18) Maistriau, L.; Dumont, N.; Nagy, J. B.; Gabelica, Z.; Derouane, E.G. *Zeolites* **1990**, *10*, 243.
(19) Afeworki, M.; Dorset, D. L.; Kennedy, G. J.; Strohmaier, K. G. *Chem. Mater*. **2006**, *18*, 1705.
(20) Valyocsik, E. W.; von Ballmoos, R. U. S. Patent 4,778,780, **1988**.
(21) Castro, M.; Garcia, R.; Warrender, S. J.; Wright, P. A.; Cox, P. A.; Fecant, A.; Mellot-Draznieks, C.; Bats, N. *Chem. Commun*. **2007**, 3470.
(22) Thompson, S. P.; Parker, J. E.; Potter, J.; Hill, T. P.; Birt, A.; Cobb, T. M.; Yuan, F.; Tang, C. C. *Rev. Sci. Inst*. **2009**, *80*, 057107.
(23) Larson, A. C.; von Dreele, R. B. *Generalised Crystal Structure Analysis System*; Los Alamos National Laboratory: Los Alamos, NM, 1998.

The structure was solved and refined using the SHELXS program and refined using the SHELXL-97 code.[24]

The morphology of the products was studied by SEM and selected area inorganic chemical analysis was performed by EDX on a JEOL JSM-5600 SEM with a tungsten filament and an Oxford INCA Energy 200 analyser. Electron diffraction was performed on a calcined sample of STA-15 using a JEOL 2010 electron microscope operating at an accelerating voltage of 200 kV. The sample was ground and deposited from a suspension in acetone onto a holey carbon grid. ED patterns were taken directly onto film. Chemical analysis for carbon, hydrogen and nitrogen was performed on as-prepared samples using a CE Instruments EA 1110 CHNS analyser.

Solid-state NMR experiments were performed on as-prepared and dehydrated, calcined STA-15 samples using a Bruker Avance III 600 spectrometer, equipped with a widebore 14.1 T magnet, yielding Larmor frequencies of 243.0 MHz for ^{31}P, 156.4 MHz for ^{27}Al and 150.9 MHz for ^{13}C. Samples were packed in conventional 4 mm ZrO_2 rotors and rotated at a rate of 10 kHz. For calcined samples, the open rotor was heated overnight at 100 °C prior to collection of the spectra. Chemical shifts are recorded in ppm relative to 85 % H_3PO_4 for ^{31}P, 1 M $Al(NO_3)_3$ (aq) for ^{27}Al and TMS for ^{13}C. For ^{13}C spectra were acquired using cross-polarization, with a contact pulse (ramped for ^{1}H) of 1 ms and ^{1}H decoupling (SPINAL32 with $\omega_1/2\pi$ = 100 kHz) applied throughout acquisition. Relative spectral intensities were analysed using the DMFIT program.[25]

Density functional theory (DFT) calculations were carried out on the $AlPO_4$ framework structure of STA-15 using the experimentally measured structure of calcined STA-15 at 290 K as a starting point. The structure was optimized and NMR parameters were calculated for ^{27}Al and ^{31}P. The CASTEP[26,27] code was used, which employs the gauge including projector augmented wave (GIPAW)[26] algorithm, to reconstruct the all-electron wave function in a magnetic field. The generalized gradient approximation (GGA) PBE functional was used and the core−valence interactions were described by ultrasoft pseudopotentials. Integrals over the Brillouin zone were performed using a Monkhorst−Pack grid with a k-point spacing of 0.04 $Å^{-1}$. Wavefunctions were expanded in planewaves with a kinetic energy smaller than the cut-off energy of 60 Ry. Calculations were performed using the EaStCHEM Research Computing Facility, which consists of 136 AMD Opteron processing cores partly connected by Infinipath high speed interconnects. Typical NMR calculation times were 78 hours using 28 processors. The isotropic chemical shift, δ_{iso}, is given by $-(\sigma_{iso} - \sigma_{ref})$, where σ_{iso}, is the isotropic shielding. Reference shieldings, σ_{ref}, of 553.2 ppm, and 280.4 ppm were used for ^{27}Al and ^{31}P, respectively, obtained from previous work.[28] The structure was geometry optimized within the CASTEP program (with all atomic positions and the unit cell dimensions allowed to vary). No symmetry restrictions were applied.

TGA was performed at 10 °C min^{-1} in air using a TA Instruments SDT 2960 thermogravimetric analyser. The N_2 adsorption isotherm at 77 K was measured for STA-15 previously calcined in O_2 at 550 °C for 12 h, using a fully automated Hiden IGA gravimetric apparatus. STA-15 was dehydrated at temperatures of 150 °C or 200 °C under vacuum (10^{-4} Torr) in the IGA instrument prior to adsorption, but this did not affect the uptake. The adsorption isotherms of toluene and n-hexane were measured by following pressure changes on a glass vacuum line of calibrated volumes fitted with PTFE taps. The solvents were dried over molecular sieves and adsorbed gases removed by freeze-thaw cycles and evacuation. The calcined STA-15 was dehydrated under a vacuum of 10^{-4} Torr and 200 °C for 3 hours prior to measuring the isotherms.

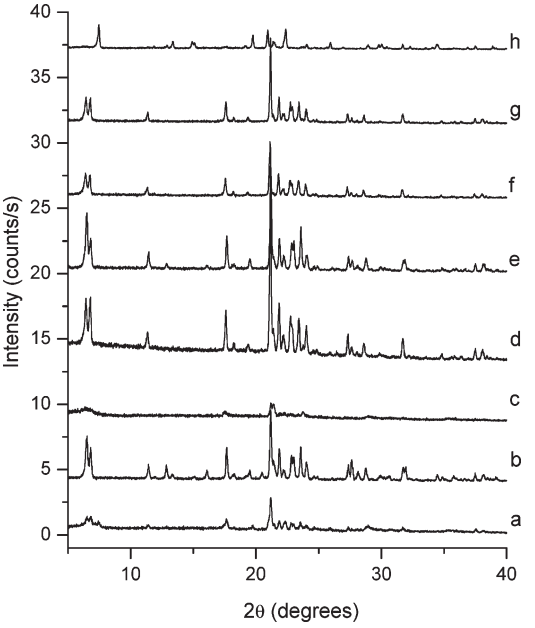

Figure 1. Powder X-ray diffraction patterns of the products of reactions a−h of Table 1. Samples d, f and g are pure STA-15.

Results and Discussion

Synthesis and Characterization of As-Prepared STA-15. Details of some of the hydrothermal syntheses (190 °C for 168 h) are given in Table 1, and powder diffraction patterns are shown in Figure 1. Using only TPAOH as a potential structure directing agent and with a gel composition $Al(OH)_3 \cdot 0.2\ H_2O/H_3PO_4/TPAOH/H_2O$ = 1:1:0.64:70 gave a mixture of the known phase $AlPO_4$-5 and a second phase, subsequently identified as a novel large pore solid and named STA-15. Reducing the Al/P ratio to 0.9 gave STA-15 with a small amount of an unidentified impurity and adding fumed silica to the reactant mixture gave STA-15 of low crystallinity. The addition of small amounts of TPP^+ (molar ratio TPP^+/P = 0.108:1) or K222 (K222/P = 0.008:1) gave highly crystalline STA-15 from silica-containing gels (yields of 40−50 % on P). (Adding K222 at higher concentrations resulted in the crystallization of $AlPO_4$-42, for which it is a known structure directing agent.[29,30]) Subsequent reactions (e, f, g) in PTFE liners previously used in the above STA-15 syntheses and subsequently washed in hot dilute nitric acid

(24) Sheldrick, G. M. SHELXL97. *Acta Cryst* **2008**, *A64*, 112.
(25) Massiot, D.; Fayon, F.; Capron, M.; King, I.; Le Calve, S.; Alonso, B.; Durand, J. O.; Bujoli, B.; Gan, Z.; Hoatson, G. *Magn. Reson. Chem.* **2002**, *40*, 70.
(26) Segall, M. D.; Lindan, P. J. D.; Probert, M. J.; Pickard, C. J.; Hasnip, P. J.; Clark, S. J.; Payne, M. C. *J. Phys. Cond. Matter* **2002**, *14*, 2717.
(27) Pickard, C. J.; Mauri, F. *Phys. Rev. B* **2001**, *63*, 245101.
(28) C. Ashbrook, S. E.; Cutajar, M.; Pickard, C. J.; Walton, R. I.; Wimperis, S. *Phys. Chem. Chem. Phys.* **2008**, *10*, 5754.
(29) Schreyeck, L.; D'Agosto, F.; Stumbe, J.; Caullet, P.; Mougenel, J. C. *Chem. Commun.* **1997**, 1241.
(30) Maple, M. J.; Philp, E. F.; Slawin, A. M. Z.; Lightfoot, P.; Cox, P. A.; Wright, P. A. *J. Mater. Chem.* **2001**, *11*, 98.

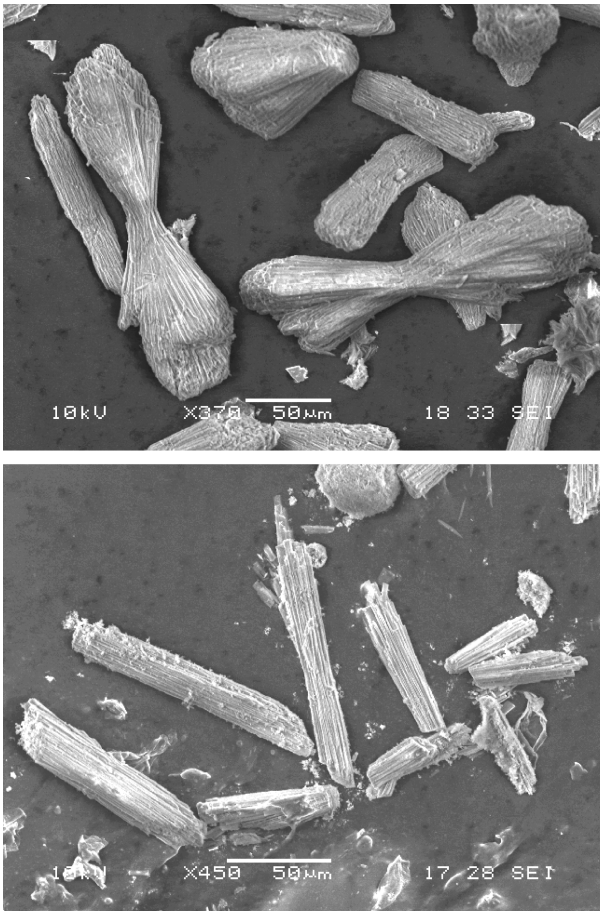

Figure 2. Representative scanning electron micrographs of STA-15 prepared in the presence of the additive TPP^+ after (below) 3 days and (above) 7 days at 190 °C.

gave pure or nearly pure STA-15 in the presence or absence of silica or organic additives, probably as a result of seeding effects because of residual STA-15 left after washing. When preparation b, with Al/P = 0.9 and H_2O/P = 70, was repeated with half the original water content, $AlPO_4$-5 crystallized instead.

After 72 h of heating the corresponding gels without organic additives, preparations b, c, and g of Table 1 gave very low yields of STA-15 (yield <5% on P), but the addition of small amounts of the bulky organic species K222 and TPP^+ (e.g. preparation d) were found to accelerate its crystallization, giving higher yields of crystalline STA-15 (yield 30 % on P).

STA-15 crystallizes as overgrown or sheaf-like bundles of long plates after 7 days, with or without species other than the Al and P sources and TPAOH (Figure 2). The most crystalline materials were prepared in the presence of silica and TPP or K222, in which preparations elongated rods showing overgrowth structure are already present after 3 days of heating, and were analyzed by single crystal diffraction. EDX analysis indicated Al/P ratios of 1:1 in the STA-15 products from a to g with very low silicon contents even for those samples prepared in the presence of silica in the gel.

^{27}Al MAS NMR of the as-prepared aluminophosphate solids (Figure 3, lower spectrum) indicates that most of

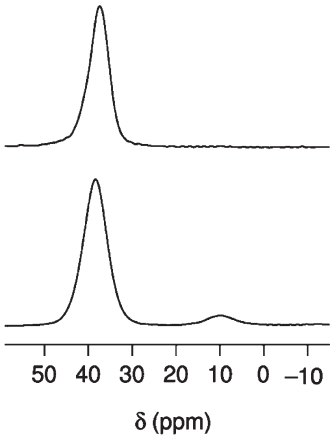

Figure 3. Solid-state ^{27}Al MAS NMR of (below) as-prepared and (above) calcined STA-15.

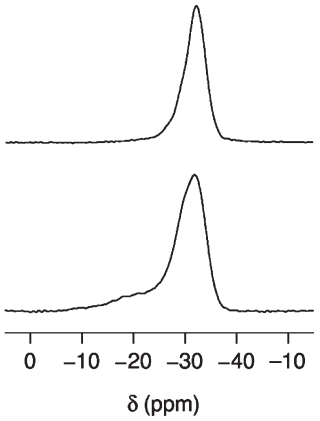

Figure 4. Solid-state ^{31}P MAS NMR of (below) as-prepared and (above) calcined STA-15.

the Al is in tetrahedral coordination ($Al(OP)_4$) (δ 38.4 ppm) with small amounts (6.7 % of the total ^{27}Al) of five-fold coordinated species (δ 9.7 ppm) and no evidence of $Al(OP)_3(OSi)$ environments, which would be observed as a shoulder on the $Al(OP)_4$ resonance. No ^{29}Si resonance was observed in the samples prepared in the presence of silicon, confirming that Si is not taken up into framework cation positions. ^{31}P MAS NMR (Figure 4) gives a sharp peak because of tetrahedral $P(OAl)_4$ at −31.1 ppm, together with a broad shoulder downfield, which makes up ~20% of the total ^{31}P signal. Similar downfield shifts of signals in the ^{31}P NMR spectra of AlPOs have previously been attributed to P atoms linked tetrahedrally (through O atoms) to Al atoms, one or more of which are five-fold coordinated.[31] The ^{13}C MAS NMR spectrum (δ 60.4, 16.5, 13.2 ppm, Supporting Information Figure S1) is consistent with TPA^+ cations being the only included organic species, even in those syntheses where other co-bases were added, and elemental analysis supports this, with an observed average C/N ratio of 11.9 (compared to 12 for TPA^+). TGA (10 °C min^{-1}, air) showed 1.4 wt % loss below 200 °C, attributed to water loss, followed by a gradual weight loss of 8.2% to 800 °C, attributed to

(31) Tuel, A.; Lorentz, C.; Gramlich, V.; Baerlocher, C. *C. R. Chim.* **2005**, *8*, 531.

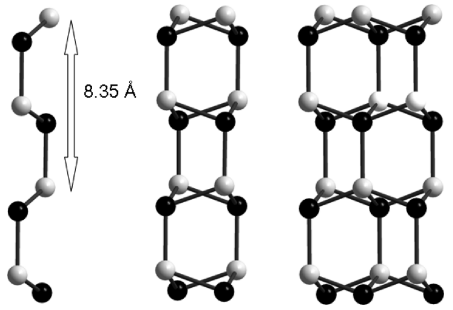

Figure 5. Left, schematic representation of the "crankshaft" aluminophosphate chain, with characteristic 8.35 Å repeat, frequently observed in aluminophosphate zeotype materials. O atoms are omitted for clarity, and closed and open circles represent Al and P atoms at the centre of tetrahedra. The connectivity between tetrahedra is indicated by solid links. Centre and right are representations of the narsarsukite chain (two linked crankshaft chains) and the double narsarsukite chain (three linked crankshaft chains) observed in aluminophosphate structures.

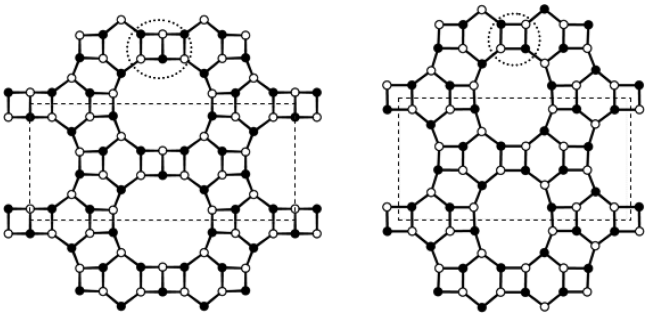

Figure 6. Schematic views of the tetrahedral connectivity in (left) $AlPO_4$-8 and (right) STA-15, in each case projected parallel to the axis of the crankshaft chains in the two structures. Al and P atoms are represented by closed and open circles and O atoms are omitted for clarity. The unit cell is outlined in each case and the double narsarsukite chains of $AlPO_4$-8 that are replaced by narsarsukite chains in STA-15 are outlined by circles.

removal of the TPA cation. A combination of NMR data, elemental analysis and TGA was used to determine the empirical charge balanced formula of as-prepared STA-15 to be $AlPO_4 \cdot (OH)_{0.06} \cdot TPA_{0.06} \cdot 0.10H_2O$ (theoretical composition, wt %, C = 6.3, N = 0.6; measured, C = 6.0, N = 0.6). On the basis of this composition, the ^{27}Al MAS NMR, in which 6.7% of the signal is from five-fold aluminium, supports a model where the hydroxyl group is terminal (where 6% of the Al would be 5-fold coordinate) rather than bridging (where 12% of the Al would be 5-fold coordinate).

Preliminary work has shown that it is possible to prepare CoAlPO STA-15 by the addition of small quantities of cobalt acetate into the reaction gel (Co/(Co + Al) = 0.06), if the preparation is seeded with a small amount of as-prepared aluminophosphate STA-15 (Table 1). The crystallization of the cobalt-bearing STA-15 phase is confirmed by (i) PXRD (with some impurity present, Supporting Information), (ii) the blue color of the STA-15 crystals, which suggest Co(II) in tetrahedral framework sites, and most importantly, (iii) selected area EDX analysis of the needle like STA-15 crystals (which have a similar morphology to the $AlPO_4$−STA-15 crystals), which indicates a framework composition of approximately $Co_{0.06}Al_{0.94}PO_4$. All subsequent characterization refers to the pure aluminophosphate version of STA-15, however.

Structure Solution of STA-15. The synchrotron X-ray powder diffraction pattern of an as-prepared sample of STA-15 (preparation d of Table 1) collected at 100 K was indexed on a body-centred orthorhombic unit cell (a = 14.799 Å, b = 27.369 Å, c = 8.347 Å). The reflection conditions ($(hk0)$, $h + k = 2n$; $(0kl)$, $k,l = 2n$; $(h0l)$, $h,l = 2n$) indicated the space group to be *Iba*2 or *Ibam*. The structure solution of STA-15 was achieved by combining X-ray powder diffraction and structure modeling. Initially, comparison of the unit cell dimensions determined from the powder data with those of known $AlPO_4$ structures indicated that the c axis (8.35 Å) is typical of $AlPO_4$ structures built from a structural unit described as the crankshaft chain, with a repeat unit of two AlO_4 and two PO_4 tetrahedra (Figure 5). For a fully ordered aluminophosphate framework, there can be no mirror plane perpendicular to a crankshaft chain so the space group must be *Iba*2. Furthermore, two of the unit cell dimensions were very close to those of the known $AlPO_4$-8[32,33] with the third shorter by a distance (~6 Å) typical of two Al−P distances. It was therefore possible to construct a structural model for STA-15 with the correct space group symmetry starting from the $AlPO_4$-8 structure, which is represented in projection along the chain axis by the connection of its tetrahedral cations (T-sites) in Figure 6. Linking the structural layers present in the $AlPO_4$-8 structure by single narsarsukite chains (Figure 5), which are made up of two crankshaft chains related by a centre of symmetry, and not by the double narsarsukite chains (Figure 5) present in $AlPO_4$-8 gives a starting structure for STA-15 consistent with the symmetry (Figure 6). Previously, the topology of this model was proposed as a theoretical structure for $AlPO_4$s during the "enumeration of four-connected three dimensional nets produced by the conversion of all edges of simple 2D nets into crankshaft chains" by Han and Smith.[34] The framework topology was produced by conversion of a 2D net with the circuit symbol (as named by Wells, appendix of paper of Smith[35]) $(46^2)_1(4.6.12)_1(4.6.12)_1(6^2 12)_1$ to a 3D net of circuit symbol (46^5), (46^5), (46^5), (6^6) and was predicted to have unit cell parameters 15 × 28 × 8.5 Å, close to those observed here. Notably, the regular alternation of up and down linkages of T-sites requires that only one 3D net can be produced from each 2D net, so that no other structures based on crankshaft chains with similar projections down the 8.5 Å axis (that might give similar diffraction patterns) are possible.

Approximate fractional atomic coordinates were determined for this model and used as a starting point for Rietveld profile analysis of the as-prepared solid. The geometries of the AlO_4 and PO_4 tetrahedra were restrained by restraining Al−O, P−O, O−O(AlO_4) and O−O(PO_4) distances to be close to 1.71 Å, 1.51 Å, 2.80 Å

(32) Dessau, R. M.; Schlenker, J. L.; Higgins, J. B. *Zeolites* **1990**, *10*, 522.
(33) Richardson, J. W.; Vogt, E. T. C. *Zeolites* **1992**, *12*, 13.
(34) Han, S.; Smith, J. V. *Acta Crystallogr* **1999**, *A55*, 332.
(35) Smith, J. V. *Am. Mineral.* **1978**, *63*, 960.

and 2.47 Å, respectively. Refinement proceeded smoothly for the framework positions and some possible positions of template atoms were included from difference Fourier maps and refined successfully, although complete TPA^+ cations were not located. The extraframework scattering was refined as C atoms at full occupancy, as part of the TPA^+ cations, although it was not possible to distinguish between C and N atoms. C−C distances were constrained to 1.50(1) Å. The best fit to the data was achieved by using the profile function of Stephens et al. for anisotropically broadened reflections.[36] Hydroxyl species coordinated to the Al cations were not located and could be disordered over many sites. The final fit to the data is shown in Figure 7, and crystallographic details of the refinement are given in Table 2. The final unit cell composition of the as-prepared material is $Al_{32}P_{32}O_{128}(OH)_{1.8}(TPA)_{1.8}\cdot 3H_2O$, where the charge balancing hydroxyl groups are coordinated to framework Al cations and there is nearly one (0.9) TPA^+ cation per channel site. The final structure of as-prepared STA-15 determined from powder data is shown in Figure 8, and the atomic coordinates are given in Table 3. Rietveld refinement of powder data at 100 K of a STA-15 sample prepared in the presence of TPP^+ was also performed, in the same way, and the details are given in Table 2 and in the Supporting Information. In this case, peak profile function 2 in GSAS was used.[37] The refinement gave a similar R_{Bragg} for the fit and similar structure parameters, with a slightly higher R_{wp}. The mean values and spreads of final Al−O and P−O lengths and the ranges of O−Al−O and O−P−O angles were similar for the two samples, Table 4, and within a reasonable range for $AlPO_4$ structures. Additional data is given in the Supporting Information and cif files.

There are four crystallographically distinct Al sites and four distinct P sites in the STA-15 structure. Like many aluminophosphates, STA-15 is built entirely of crankshaft chains and possesses the same layered building unit as $AlPO_4$-8, although in STA-15 these are linked via narsarsukite rather than double narsarsukite chains. Channels running parallel to the *c* axis are limited by 12-membered rings (12 tetrahedral cations and 12 O atoms − 12MRs). The channels are lined exclusively by 6MRs and so are not connected. Notably the Al−O−P angles linking tetrahedra along *c* show larger values (159−175°) than those in the plane of the layers (137−165°) (as determined from the X-ray powder diffraction data).

In parallel with these powder diffraction studies, it was possible to perform single crystal diffraction on small crystals of as-prepared STA-15 prepared after 72 h crystallization time. Although the data was not of very high quality, due to the small size and the stacked overgrowth nature of the crystals, they confirm the unit cell, space group and structural model obtained from powder diffraction.

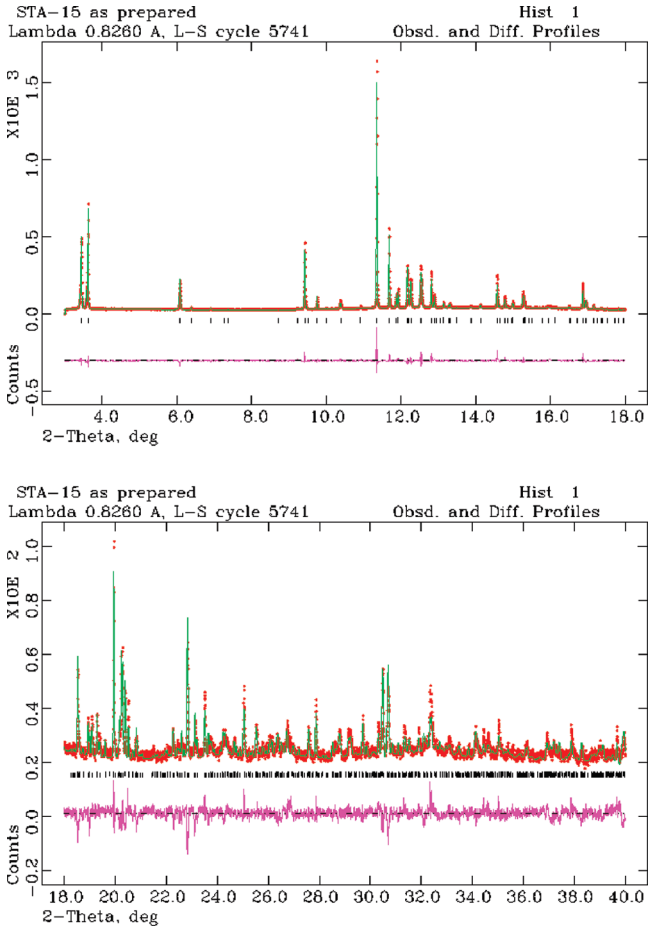

Figure 7. Rietveld refinement plot of as-prepared $AlPO_4$ STA-15, sample d, measured at 100 K, showing measured data (red), fitted data (green), and the difference plot (purple).

STA-15 is, to our knowledge, the fourth aluminophosphate discovered with a 1D 12MR channel network in which the channels are not connected, the others being $AlPO_4$-5,[38] AlPO-31,[39] and $AlPO_4$-36.[40,41] The structure of STA-15 is compared with that of the well known $AlPO_4$-5 in Figure 9. Both are made up only of crankshaft chains and contain one dimensional 12MR pore systems. In $AlPO_4$-5, the structure is made up only of narsarsukite chains, whereas in STA-15, there are also single crankshaft chains. The channels of both are lined only with 6MRs, and the main difference in the channel geometry between the two structures is that the channels in $AlPO_4$-5 are circular in cross section (7.3 × 7.3 Å), whereas those in STA-15 are strongly elliptical (8.7 × 5.7 Å). The channels of $AlPO_4$-36 (which does not contain crankshaft chains) show intermediate cross-sectional ellipticity (7.5 × 6.5 Å) and the channels of $AlPO_4$-31, which are bounded by nonplanar 12MRs, are circular and much smaller in cross-section (5.4 × 5.4 Å).

(36) Stephens, P. W. *J. Appl. Crystallogr.* **1999**, *32*, 281.
(37) (a) Howard, C. J. *J. Appl. Crystallogr.* **1982**, *15*, 615. (b) Thompson, P.; Cox, D. E.; Hastings, J. B. *J. Appl. Crystallogr.* **1987**, 20,79.
(38) Bennett, J.M.; Cohen, J.P.; Flanigen, E.M.; Pluth, J.J.; Smith, J.V *ACS Symp. Ser.* **1983**, *218*, 109.
(39) Bennett, J. M.; Kirchner, R. M. *Zeolites* **1992**, *12*, 338.
(40) Smith, J.V.; Pluth, J.J.; Andries, K.J. *Zeolites* **1993**, *13*, 166–169.
(41) Wright, P. A.; Natarajan, S.; Thomas, J. M.; Bell, R. G.; Gai-Boyes, P. L.; Jones, R. H.; Chen, J. *Angew. Chem., Int. Ed. Engl.* **1992**, *31*, 1472.

Table 2. Crystallographic Details of Structure Refinements of As-Prepared and Calcined STA-15 (Preparations d and f, Table 1) against Powder X-ray Diffraction Data

	sample d, as-prepared	sample d, calcined	sample f, as-prepared	sample f, calcined
experimental unit cell composition	$Al_{32}P_{32}O_{128}(OH)_{1.8}$ $TPA_{1.8}\cdot 3H_2O$	$Al_{32}P_{32}O_{128}$	$Al_{32}P_{32}O_{128}(OH)_{1.8}TPA_{1.8}\cdot 3H_2O$	$Al_{32}P_{32}O_{128}$
diffractometer	Synchrotron, I11, DLS	Stoe STAD i/p	Synchrotron, I11, DLS	Synchrotron, I11, DLS
wavelength	0.826019	1.54056	0.827267	0.827267
temperature (K)	100(2)	290(2)	100(2)	100(2)
crystal system	orthorhombic	orthorhombic	orthorhombic	orthorhombic
space group	*Iba*2 (No. 45)	*Iba*2 (No. 45)	*Iba*2 (No. 45)	*Iba*2 (No. 45)
a (Å)	14.7953(1)	14.7696(6)	14.8022(1)	14.7967(1)
b (Å)	27.3634(3)	27.6373(11)	27.3306(2)	27.5248(3)
c (Å)	8.34464(6)	8.3580(2)	8.34870(4)	8.32555(4)
V (Å^3)	3378.31(7)	3411.6(3)	3377.47(5)	3390.79(6)
2θ range of refinement (deg)	2−40	5−80	2−40	2−35
R_{wp}, R_p , R_B (%)	6.8, 5.2, 8.9	9.2, 6.6, 7.2	10.1, 6.4, 8.2	9.9, 7.5, 8.6
χ^2	4	2.9	1.6	1.6

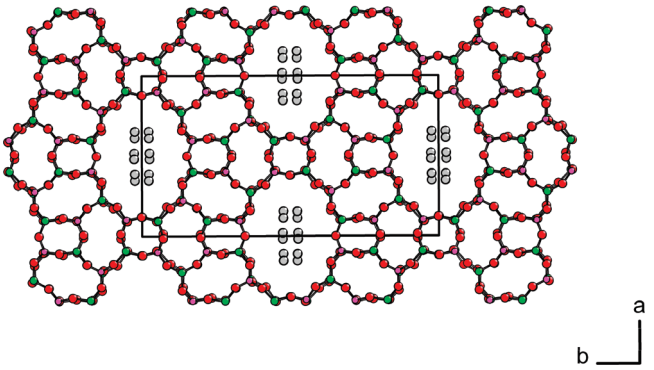

Figure 8. Structure of as-prepared $AlPO_4$-5 STA-15, viewed down z and with the unit cell outlined. (Al atoms in green, P atoms in purple, O atoms in red. Extra framework scattering (C, N) atoms depicted in gray.).

Table 3. Fractional Atomic Coordinates and Displacement Parameters for As-Prepared $AlPO_4$ STA-15 (Sample d) at 100 K

atom	x	y	z	frac	U_{iso} (Å^2)
P1	0.9024(5)	0.7831(2)	0.1671(8)	1	0.037(1)
P2	0.9062(5)	0.6702(2)	0.6624(8)	1	0.037(1)
P3	0.7203(4)	0.6388(2)	0.1570(7)	1	0.037(1)
P4	0.3978(4)	0.5526(2)	0.1563(9)	1	0.037(1)
Al1	0.9068(5)	0.7796(2)	0.7882(7)	1	0.037(1)
Al2	0.8999(5)	0.6739(2)	0.2838(7)	1	0.037(1)
Al3	0.5930(5)	0.5547(24)	0.2780(8)	1	0.037(1)
Al4	0.2714(6)	0.6338(2)	0.2834(7)	1	0.037(1)
O1	0.8848(8)	0.7339(2)	0.2405(11)	1	0.037(1)
O2	0.9906(6)	0.8026(3)	0.2295(13)	1	0.037(1)
O3	0.8253(7)	0.8156(3)	0.2152(13)	1	0.037(1)
O4	0.9008(6)	0.7799(4)	0.9902(7)	1	0.037(1)
O5	0.8928(8)	0.7214(2)	0.7196(11)	1	0.037(1)
O6	0.8403(5)	0.6354(3)	0.7408(11)	1	0.037(1)
O7	0.8980(6)	0.6670(3)	0.4854(7)	1	0.037(1)
O8	1.0000(5)	0.6528(3)	0.2074(13)	1	0.037(1)
O9	0.8179(5)	0.6375(3)	0.2039(11)	1	0.037(1)
O10	0.6770(7)	0.6861(3)	0.2034(12)	1	0.037(1)
O11	0.7135(6)	0.6297(4)	0.9830(6)	1	0.037(1)
O12	0.6737(7)	0.5965(3)	0.2349(11)	1	0.037(1)
O13	0.4856(5)	0.5715(3)	0.2227(13)	1	0.037(1)
O14	0.3798(6)	0.5014(2)	0.2079(12)	1	0.037(1)
O15	0.3175(6)	0.5834(3)	0.1960(12)	1	0.037(1)
O16	0.4077(6)	0.5495(3)	0.9807(8)	1	0.037(1)
C1	0.0188(9)	0.5258(3)	0.7911(22)	1	0.037(1)
C2	0.1120(10)	0.5238(9)	0.8662(24)	1	0.037(1)
C3	0.1538(12)	0.4766(10)	0.8188(28)	1	0.037(1)

Given the large synthetic effort made in the synthesis of $AlPO_4$-based materials, particularly using commercially available templates, it was surprising to us that a novel solid had been prepared using TPA^+ as an SDA. For pure aluminophosphate gel preparations, our results indicate that at 190 °C, both $AlPO_4$-5 and STA-15 can crystallize, with the crystallization of STA-15 favored by higher water content ($H_2O/P = 70$) and an Al/P ratio less than 1 (0.9). Previous reported aluminophosphate preparations had used 150 °C as a crystallization temperature and lower water contents ($H_2O/P = 20-50$) and had given $AlPO_4$-5[4] and $AlPO_4$-5/$AlPO_4$-40 mixtures.[15]

The effect of the addition of silica in our preparations is to reduce the nucleation rate of the (S)APO-5 relative to that of STA-15, rather than becoming incorporated in the STA-15 structure. A similar effect was observed in the co-crystallization of SAPO-40 and SAPO-5 by Dumont et al.,[16] where higher silica contents in the gel favored SAPO-40 over SAPO-5. Using similar crystallization temperatures but a lower H_2O/P ratio (35) than in our work, Si/(Si + Al + P) ratios above 0.1 gave SAPO-40. Interestingly, over a narrow range of added SiO_2 (Si/(Si + Al + P) ≈ 0.09), a complex mixture of SAPO-5, SAPO-40, and a third, unidentified phase was reported. The authors were unable to obtain this material in pure form, but, on the basis of some of the reflections attributed to this phase, it seems likely that this impurity could have been the material we report as STA-15 here, and that we have achieved its synthesis as a pure phase by increasing the water content, reducing the Al/P ratio, and the addition of organic additives such as K222 and TPP^+. We speculate that the effect of these organic additives is to preorganize species in the aluminophosphate gel and to favor the nucleation of STA-15 rather than $AlPO_4$-5. They are too large to become incorporated in either of the co-crystallizing zeotypes.

Structure and Properties of Calcined STA-15. Calcination of as-prepared STA-15 in flowing oxygen (550 °C, 12 h) gave a white crystalline solid without loss of crystallinity, as shown from the PXRD (Figure 10).[27]Al and [31]P MAS NMR spectra of the calcined material (Figures 3 and 4) give single resonances indicative of tetrahedral environments, $Al(OP)_4$ (δ 37.5 ppm) and $P(OAl)_4$ (δ −32.0 ppm). This indicates that hydroxyl species coordinated to the framework aluminium were removed in this process, leaving a fully tetrahedrally-connected $AlPO_4$ framework without organic species in the pores, but

Table 4. Bond Lengths and Angles from Refined Structures of STA-5 in As-Prepared and Calcined Forms

	STA-15 sample d	STA-15 sample f	STA-15 sample d	STA-15 sample f
preparation	as-prepared	as-prepared	calcined	calcined
X-rays	Synchrotron	Synchrotron	Lab	Synchrotron
temperature/K	100	100	290	100
mean Al−O (esd)/Å	1.700(10)	1.698(16)	1.703(9)	1.702(11)
range Al−O/Å	1.684−1.717	1.677−1.729	1.690−1.721	1.683−1.717
mean P−O/Å	1.495(12)	1.495(17)	1.501(10)	1.499(13)
range P−O/Å	1.476−1.514	1.473−1.516	1.488−1.521	1.480−1.518
mean O−Al−O (deg)	109(3)	109(2)	109(2)	109(3)
range O−Al−O (deg)	105.7−114.5	106.9−112.6	106.6−112.5	104.0−114.0
mean O−P−O (deg)	109(3)	109(2)	109(2)	109(2)
range O−P−O (deg)	104.5−114.3	107.0−112.9	106.9−113.3	105.7−113.3

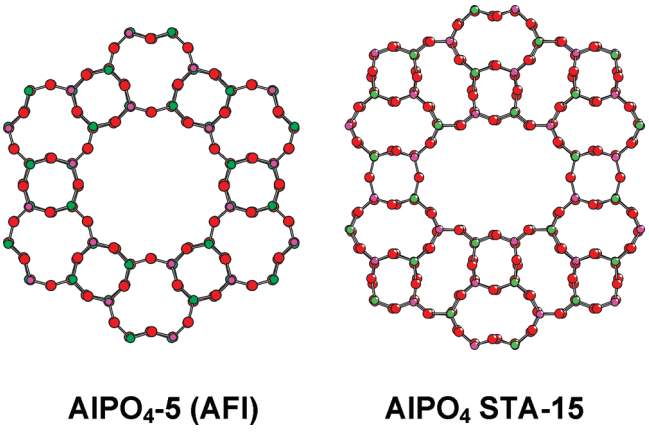

Figure 9. Comparison of the cross sections of the channels in $AlPO_4$-5 and STA-15, viewed down the channel axis along the crankshaft chains in each case. (Color scheme as in Figure 8.).

crystallographically distinct framework Al or P sites were not resolved in the NMR spectra. Electron diffraction studies of calcined STA-15 (Electron diffraction reflection conditions [100] $k,l = 2n$; [010] $h,l = 2n$) confirmed the space group to be *Iba*2 (Supporting Information Figure S5) and did not show the type of superstructure reflections along c^* corresponding to a doubling of the c axis that have been observed in template-free $AlPO_4$-8.[42] No electron diffraction patterns were observed down the [001] axis of STA-15, because the c-axis runs along the long axis of the long thin crystals. The sample is beam sensitive and no high resolution TEM images were recorded.

The structure of calcined samples d and f of STA-15 were therefore refined against laboratory (290 K) and synchrotron (100 K) X-ray powder diffraction data using the same structural model, and restraining framework atom−atom distances as in the refinement of the as-prepared material. Profile 2 of GSAS was used in the Rietveld fit. (Table 2 and Supporting Information). The fit to the laboratory x-ray data of calcined STA-15 (sample d) is shown in figure 11. The framework structure of calcined STA-15 is similar to that of the as-prepared solid. The free pore sizes of the calcined solids are measured as 5.9 × 8.8 Å at 100 K and 6.0 × 8.6 Å at 290 K. Direct comparison of $AlPO_4$ STA-15 in the as-prepared and calcined states at 100 K (Table 2) shows that upon calcination the volume increases by 0.4%, because

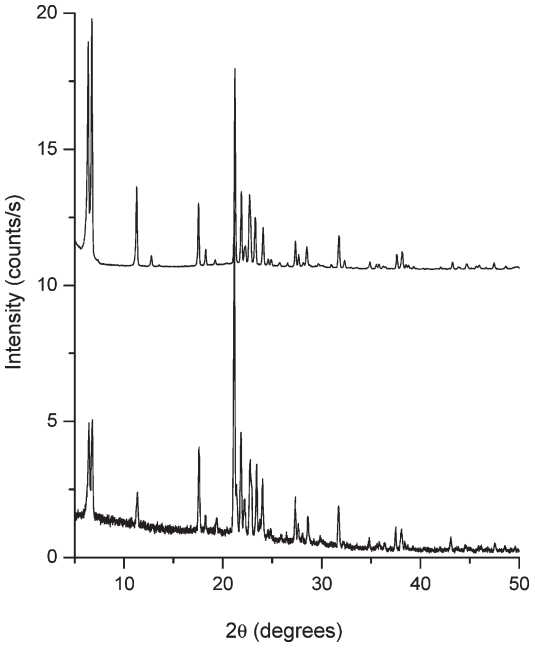

Figure 10. Laboratory X-ray diffraction profile (λ = 1.54056 Å) of calcined STA-15 (above) compared with that of the as-prepared solid (below).

of an expansion along b (0.71%), while a and c decrease (by 0.04% and 0.28%, respectively).

The complexity of the unit cell (4 independent Al sites, 4 P sites and 16 O sites, none on special positions, giving 72 variable fractional atomic coordinates) requires the refinements of STA-15 to be restrained. To support the symmetry assignment and to help understand the unresolved ^{27}Al and ^{31}P MAS NMR spectra given the presence of 4 different Al and P sites, the $AlPO_4$ framework model was optimized without symmetry constraints by DFT methods, and the ^{31}P and ^{27}Al NMR parameters were calculated from the optimized structure, as described in the Experimental Section. The final optimized structure retained orthorhombic *Iba2* symmetry, supporting the structure refinement, with a, b, and c lattice parameters around 2% larger than experimental, as commonly seen in DFT simulations. Upon optimization of the structure the T−O bond distances and O−T−O bond angles become more similar both within TO_4 tetrahedra and between the different tetrahedra. ^{27}Al isotropic chemical shifts of the 4 sites were calculated in a narrow 4 ppm range (between 33.4 and 37.2 ppm) and with similar C_Q values (between 2.5 and 3.6 MHz). These appear

(42) Withers, R. L.; Liu, Y. *J. Solid-State Chem.* **2005**, *178*, 2647.

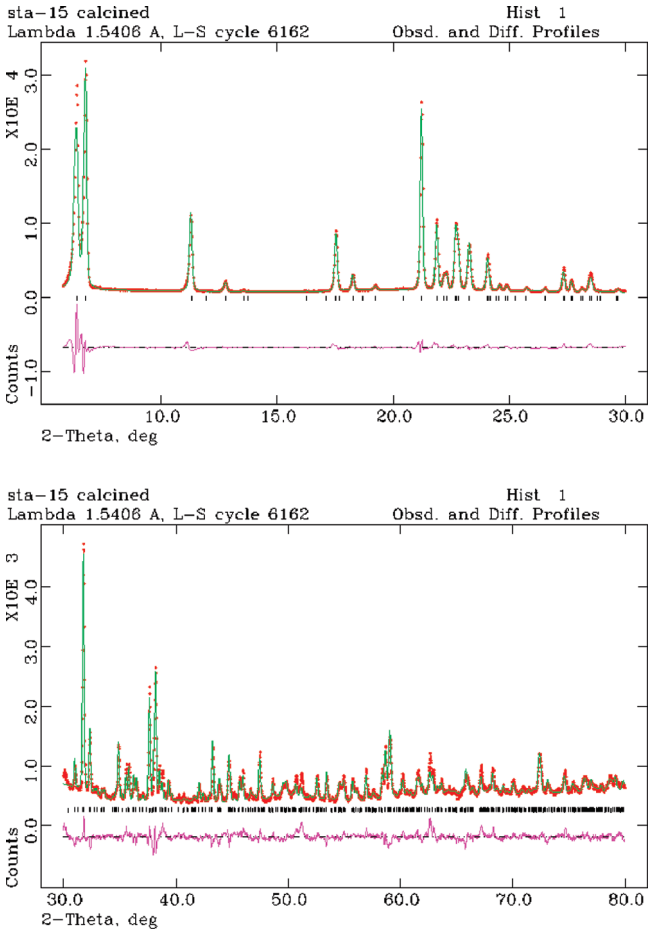

Figure 11. Rietveld refinement plot of calcined $AlPO_4$ STA-15, sample *d*, measured at 290 K, showing measured data (red), fitted data (green), and the difference plot (purple).

unresolved in the spectrum, although the relatively narrow line (given Al is quadrupolar) is in agreement with small quadrupolar couplings. Similarly, the spread in ^{31}P isotropic chemical shifts calculated from the minimized structure (−34.7 to −38.7 ppm) is within the 5 ppm halfwidth of the relatively broad single resonance observed experimentally. Details are given in the Supporting Information.

Once calcined, STA-15 is porous, and gives a type I adsorption isotherm with N_2 at 77 K, showing an uptake of 9 wt % at p/p_o = 0.15, corresponding to a pore volume of around 0.11 $cm^3\ g^{-1}$. This is lower than the corresponding pore volume reported for $AlPO_4$-5 (0.18 $cm^3\ g^{-1}$),[3] but this is in part because of the lower framework density and more circular channel cross section of $AlPO_4$-5. The crystallographic structure indicates that calcined STA-15 should be able to adsorb n-alkanes and monoaromatic hydrocarbons. To prove that the channels in the structure are accessible to larger molecules, and not blocked by structural faulting or residual carbonaceous species, the adsorption of *n*-hexane and toluene was measured at 297 K and found to achieve 0.48 and 0.69 mmol g^{-1}, respectively, in each case measured at p/p_o of 0.10. Adsorption isotherms are given in the Supporting Information.

Conclusions

The novel large pore aluminophosphate STA-15 crystallizes using the TPA^+ cation as a structure directing agent. The SDA is included within the channels and the charge balancing hydroxyl groups coordinate to framework Al to increase its coordination to 5-fold. STA-15 is the fourth $AlPO_4$ known with a one dimensional channel system bounded by 12MRs and with unconnected channels, the others being $AlPO_4$-5, $AlPO_4$-31, and $AlPO_4$-36. The cross-sectional dimensions in STA-15 are the most strongly elliptical of the structure types. The framework, which is built up entirely of crankshaft and narsarsukite chains, is closely related to that of $AlPO_4$-8 because it possesses the same type of complex layers parallel to these chains (along *c*), but these are linked via narsarsukite rather than double narsarsukite chains.

The synthesis of the large pore molecular sieve STA-15 using the tetrapropylammonium cation as a structure directing agent emphasizes the complexity of the crystallization process for aluminophosphates, where small changes in reactant ratios determine which phase crystallizes. In particular, it is remarkable that the STA-15 material had not previously been reported, given the ready availability of the template and considerable synthetic efforts in the $AlPO_4$ and SAPO systems, although it may have been observed previously as a minor impurity in the attempted synthesis of SAPO-40. Higher water contents and an Al/P ratio of 0.9:1 in the gel favor the crystallization of STA-15 over $AlPO_4$-5 and are thought to be the important factors in the crystallization of this phase. Furthermore, the addition of silica and bulky organic cations to the gel have the effects of increasing the purity of the product phase and accelerating the synthesis, respectively, but they are not included in the framework or in the channels, respectively.

The stability and resultant microporosity of STA-15 suggest that, once prepared with divalent metals doped into the aluminium sites, it could be an attractive catalytic material in acid and selective oxidation catalysis, given the strong performance in these reactions of $AlPO_4$-5 doped with metal cations. The markedly elliptical pore geometry of STA-15 could offer alternative shape selectivities from exhibited by $AlPO_4$-5-based catalysts. Initial results indicate that Co(II) can be incorporated into the framework and current efforts are ongoing to measure the catalytic properties of this material and also to find conditions under which the STA-15 structure is able to undergo framework substitution with other metals, such as magnesium, manganese, and iron, and measure the catalytic properties of all these solids.

Supporting Information Available: Supporting information includes ^{13}C MAS NMR spectrum, CIF files, and structural data for PXRD and SXRD data, additional Rietveld plots, TGA, electron diffraction patterns, details of CASTEP refinement and adsorption isotherms. This material is available free of charge via the Internet at http://pubs.acs.org.

Acknowledgment. We gratefully acknowledge the EPSRC for funding (VS, PAW, SEA, EP/EO41825/1), Professor Chiu C. Tang for assistance at the I11 beamline at the Diamond Light Source (DLS) and DLS for beamtime.